Single and multi-user cooperative MIMO in a measured urban macrocellular environment

Lau, Buon Kiong; Jensen, Michael A.; Medbo, Jonas; Furuskog, Johan

Published in:
IEEE Transactions on Antennas and Propagation

DOI:
10.1109/TAP.2011.2173443

2012

Document Version:
Peer reviewed version (aka post-print)

Single and Multi-user Cooperative MIMO in a Measured Urban Macrocellular Environment

Buon Kiong Lau, *Senior Member, IEEE*, Michael A. Jensen, *Fellow, IEEE*, Jonas Medbo, *Senior Member, IEEE*, and Johan Furuskog

***Abstract*—We study the potential benefits of cooperative multiple-input multiple-output signaling from multiple coherent base stations with one or more mobile stations in an urban macrocellular environment at 2.66 GHz. The analysis uses fully-coherent measurements of the channel from three base stations to a single mobile station equipped with four antennas. The observed channels are used to explore the gains in capacity enabled by cooperative base station signaling for point-to-point and multi-user communications. The analysis shows that for point-to-point links, the average capacity for cooperative signaling is 53% higher than that achieved for a single base station. For downlink and uplink communication with three mobile users, cooperative signaling using practical algorithms yields average sum rate increases of 91% and 63%, respectively.**

***Index Terms*—MIMO systems, Cooperative systems, Multiuser channels**

I. Introduction

While multiple-input multiple-output (MIMO) technology has demonstrated the potential for offering significant improvements in spectral efficiency for wireless communication, realization of these gains depends on the communication environment. For example, in cellular systems, compact device sizes at the mobile station (MS) limit the number of antennas that can observe independent fading [1]–[3]. At the base station (BS), the elevated position and sectorized nature of the antennas lead to limited observed angular spread, again limiting the benefit of multiple antennas for reasonable inter-element spacing.

While work has been accomplished to limit coupling and improve performance for compact element spacing at the MS [2], less work has addressed the issue of limited angle spread at the BS. One potential solution to this problem, however, involves using multiple BS sites working cooperatively, a solution that also potentially enables significant benefit in terms of interference control in multi-user signaling [4]–[6]. At its simplest level, such coordination involves scheduling based on awareness of interference created by multiple BS sites [7], although more sophisticated cooperation is also possible. For example, the benefit of cooperative BS communication has been studied in the context of determining the channel and shadowing correlation properties for multiple BS sites and a single MS [8], [9], although [9] did not achieve coherence across the multiple BS sites and the equipment in [8] led to phase uncertainties in the measurements. The pioneering work in [10], while using incoherent measurements from multiple BSs, uses a statistical analysis based on the low correlation between the channels [11] from the different BSs to allow exploration of the point-to-point and multi-user capacity assuming BS coherence in a campus environment at 5.2 GHz. Also, recent time-synchronized multi-BS and multi-MS measurements demonstrate the associated interference characteristics and are used to discuss some implications of cooperative MIMO signaling for multiple users in a limited fashion [12], although here the results are for a microcellular environment.

More recent work has focused on coherent channel measurements either from multiple BS sectors or from multiple BSs [13]. For example, the work in [14] develops cooperative communication for MIMO downlink communication and demonstrates its performance using coherent measured channels from two sectors at the same BS site. Some experimental data from multiple BSs in a cooperative environment are also reported in [15], although the focus of this work is on comparing the behaviors of channel eigenvalues predicted using ray tracing and observed in the channel measurements. Since the initial submission of the present paper, new results have appeared in the literature showing the impact of BS cooperation in several scenarios based on coherent multi-cell measurements [16], [17].

This paper reports on the analysis of fully-coherent measurements from three BS sites to a single MS in a macrocellular environment, measurements that complement those that have been recently reported. The observed channels are first used to explore the gains achieved with cooperative MIMO signaling to a single user. This analysis shows that channel gain imbalance plays a dominant role in determining the measured multi-BS capacity, consistent with conventional understanding, and that BS cooperation leads to an increase in average capacity of 53% over that achieved using a single BS. In places where all base stations contribute nearly equal signal power to the MS, this increase in average capacity can exceed 100%. We then turn our attention to the performance of cooperative MIMO for multi-user communications involving two and three MSs for both the downlink or broadcast channel (BC) and the uplink or multiple access channel (MAC) [5] based on different practical signaling strategies over the ob-

This work was supported in part by Telefonaktiebolaget LM Ericssons Stiftelse för Främjande av Elektroteknisk Forskning, VINNOVA under Grant 2008–00970, and in part by the U. S. Army Research Office under the Multi-University Research Initiative (MURI) Grant # W911NF-07-1-0318.

B. K. Lau is with the Department of Electrical and Information Technology, Lund University, Box 118, SE-221 00 Lund. Sweden, email: bkl@eit.lth.se

M. A. Jensen is with the Electrical and Computer Engineering Department, Brigham Young University, Provo, UT 84602, email: jensen@byu.edu

J. Medbo and J. Furuskog are with Ericsson Research, Ericsson AB, SE-164 80 Stockholm, Sweden, email: {jonas.medbo,johan.furuskog}@ericsson.com

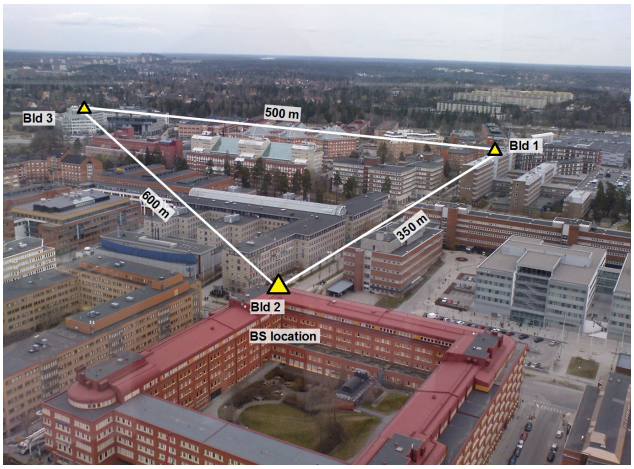

Figure 1. Birds eye view of measurement environment.

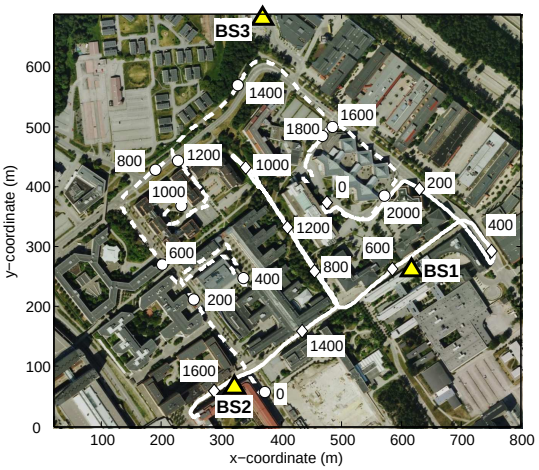

Figure 2. Location of BSs and routes 1 (- -) and 2 (–) traveled by the MS. Distances in meters from the starting points are indicated by circles and diamonds for routes 1 and 2, respectively.

served channels. This analysis shows that cooperative MIMO signaling can provide an average multi-user throughput that is up to 91% higher than that achievable using more traditional multiple-access strategies under favorable channel conditions.

One important area within this field of cooperative BS communication is the development of models that can predict the achievable performance. Some of the findings in this work demonstrate that traditional channel models can explain the key behaviors observed in cooperative BS channels provided that the models include key properties of the link gains, which is a useful observation for future channel model development. However, a key challenge is knowing the typical distribution of these link gains in practical implementation scenarios and validating any developed models against measured observations. The measurements reported here therefore provide critical understanding that will assist in the development of models appropriate for cooperative BS communication.

II. Measurement Setup

The considered urban macrocell environment is the built up area within Kista (also called "Mobile Valley"), Stockholm, Sweden, depicted in Fig. 1. Three BS sites were selected that emulate a realistic cellular deployment topology. At each BS, a single antenna mounted a few meters above the average rooftop level of approximately 25 m transmits a linearly-polarized (45° from vertical) signal. The main lobe of each antenna pattern is pointed downwards between 6° and 8° from horizontal and approximately towards the centroid of the triangle formed by the three BS sites. The MS consists of two dipole and two loop antennas mounted on the top of a measurement van as a square array with an inter-element spacing of approximately 30 cm, which is 2.6 wavelengths at the excitation frequency.

Measurement of the channel between all three BS and four MS antennas is accomplished using the Ericsson channel sounder that is based on a prototype for LTE [18] but with a custom frame structure and rate. A single transmit unit generates orthogonal frequency-division multiplexing (OFDM) channel sounding symbols that are distributed to the antennas at the three BS sites using RF-over-fiber equipment. To avoid problems with non-orthogonality of the OFDM symbols due to the MS mobility, the transmissions from these three BS antennas are time multiplexed at the symbol level.

The MS uses four parallel receiver chains to simultaneously down-convert the signals from the four receive antennas. Disciplined rubidium clocks (Stanford Research Systems, PRS10) at the transmitter and receiver provide a highly accurate synchronization (Allan standard deviation less than 10^{-12}) between the BS and the MS. Based on this timing reference, error in the measured propagation distance over all routes is less than 1 m. The resulting system generates a full 4×3 MIMO channel matrix at a rate of 1500 observations per second (based on 0.667 ms probing frames), but because of bandwidth limitations between the system and the storage medium, the observations are stored at a rate of 190 channels per second, providing high spatial resolution given the maximum van speed of 30 km/hr. All of the parameters used in the measurements are provided in Table I.

The measurements consist of data from two different routes, each requiring approximately 9 minutes of measurement time. The routes include regions of line-of-sight (LOS), obstructed line-of-sight (OLOS), and non-line-of-sight (NLOS) propagation. The position data for each channel sample is logged using a GPS receiver. Figure 2 shows the two routes along with markers indicating the distance traveled along each route and the positions of the base stations. The observed signal-to-noise ratio (SNR) computed by extracting the signal and noise powers from the channel impulse response is 28 dB on average, with the SNR for the strongest BS-to-MS link always above 22 dB and rarely below 25 dB.

We emphasize that the unique feature of this data is the coherence between the measurements from the different BSs, a feature that allows us to determine the impact of BS cooperation. Throughout this discussion, several reference cases will

Table I
SPECIFICATIONS FOR THE ERICSSON CHANNEL SOUNDER

Parameter	Value
Center Frequency	2.66 GHz
Bandwidth	19.4 MHz
Frequency bins	432
Transmit power	36 dBm
Channel acquisition rate	190 channels/s
Number of BS	3
BS antenna	1 Kathrein (18 dBi 45° polarized)
MS antenna	2 dipoles + 2 magnetic loops

be presented where the network must match a BS to one or more MSs, a pairing that requires some level of cooperation among the BSs. However, when the term *cooperative BS* is used, it explicitly refers to the case where the BSs jointly and coherently participate in the communication to the MS.

III. POINT-TO-POINT SIGNALING (MACRODIVERSITY)

We first study the communication between $N_{\rm B}$ cooperative BSs and a single MS with $N_{\rm r}$ antennas. Let $\widehat{\mathbf{H}}[f]$ represent the measured $N_{\rm r} \times N_{\rm B}$ multi-BS (MIMO) channel matrix at the fth frequency with ith column $\hat{\mathbf{h}}_i[f]$ representing the $N_{\rm r} \times 1$ single-input multiple-output (SIMO) link from the ith BS. Each channel matrix is normalized so that the average of the channel power gains for the strongest BS-to-MS link is unity, or $\mathbf{H}[f] = \sqrt{N_{\rm r}/\beta_{\rm P}}\ \widehat{\mathbf{H}}[f]$ where

$$\beta_{\rm P} = \max_i \{\beta_i\} = \max_i \left\{ \frac{1}{N_{\rm f}} \sum_{f=1}^{N_{\rm f}} \left\| \hat{\mathbf{h}}_i[f] \right\|_F^2 \right\}, \qquad (1)$$

$N_{\rm f}$ represents the number of frequencies, and $\|\cdot\|_F$ indicates a Frobenius norm. If P represents the total power transmitted and if the additive noise is modeled as a zero-mean, unit-variance complex Gaussian random process, then with this normalization P can be considered the average single-input single-output (SISO) SNR observed on the strongest BS-to-MS link [19]. The point-to-point capacity at each location averaged over the $N_{\rm f}$ frequencies and assuming that the base stations do not possess channel state information (CSI) is then given by

$$C_{\rm P} = \frac{1}{N_{\rm f}} \sum_{f=1}^{N_{\rm f}} \log_2 \left[\mathbf{I} + \frac{P}{N_{\rm B}} \mathbf{H}[f] \mathbf{H}^{\dagger}[f] \right], \qquad (2)$$

where where $\mathbf{I}$ is the identity matrix and $\{\cdot\}^{\dagger}$ indicates a conjugate transpose. We perform capacity analysis assuming a reference SNR of 10 dB, which is at least 10 dB below the SNR observed in the measurements.

Figure 3 plots the point-to-point capacity performance of the best single BS-to-MS link and the cooperative communication using all BS-to-MS links for route 1 shown in Fig. 2. To achieve improved visual clarity in this plot, the results are smoothed in the displacement variable with a moving average filter over a window of 10 wavelengths and down-sampled. These results demonstrate that BS cooperation provides significant potential capacity performance gain, particularly in regions where the MS lacks a clear view to a single (and therefore dominant) BS, such as for positions between 300 and 700 m or 900 and 1200 m. As a reference, the average capacity achieved when the channel coefficients are modeled as independent identically distributed (i.i.d.) zero-mean complex Gaussian random variables with 10 dB SISO SNR is indicated by the black triangle on the plot, revealing that the capacity falls short of what is achievable under ideal propagation conditions.

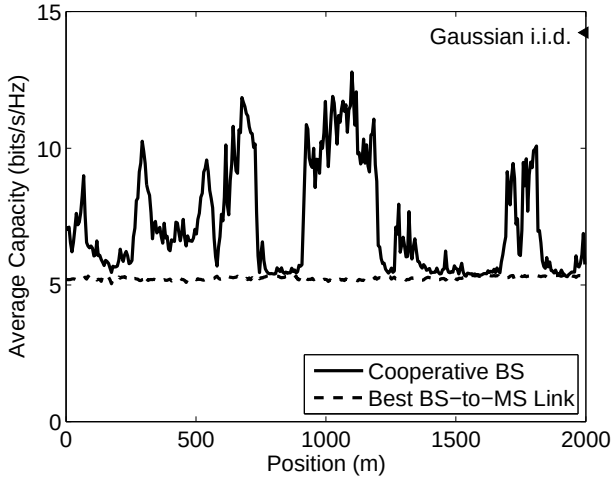

Figure 3. Average capacity for the best BS-to-MS link and for cooperative capacity using all BS links for the MS on route 1.

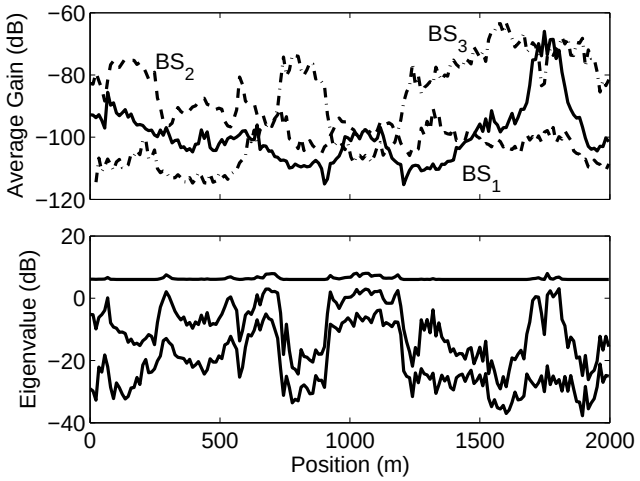

Figure 4. Average channel gains β_i for the three BSs and the dominant three eigenvalues of $\mathbf{H}[f]\mathbf{H}[f]^{\dagger}$ for the MS on route 1.

Figure 4 shows the average channel gains β_i for the three BSs as well as averages of the largest three eigenvalues of $\mathbf{H}[f]\mathbf{H}[f]^{\dagger}$ as a function of position along route 1. Comparison of these results with the capacity in Fig. 3 shows that the dominant three eigenvalues and the capacity are largest when the channel gains are nearly equal since all three BSs can effectively participate in the communication. A similar yet less dramatic capacity increase occurs when two BSs enjoy a strong link to the MS, such as for MS positions between 1700 and 1800 m.

The point that cooperative communication provides gains

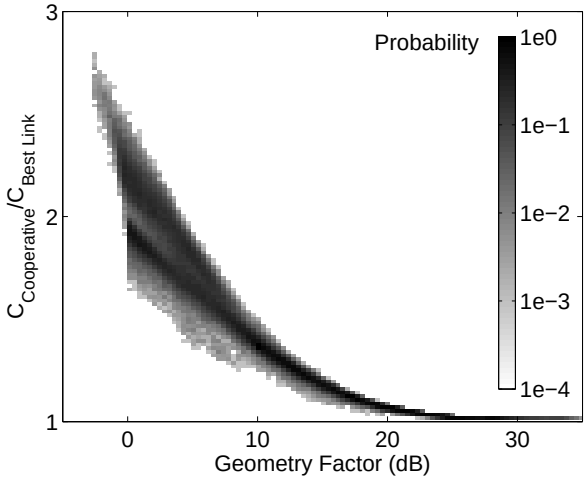

Figure 5. Two dimensional pdf of the 3GPP geometry factor and increase in the average cooperative capacity relative to the average capacity of the best BS-to-MS link for all channels in routes 1 and 2.

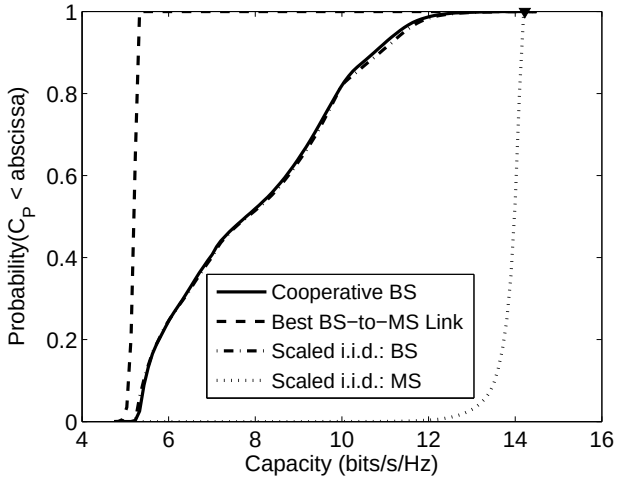

Figure 6. CDF of the capacity for the channels on routes 1 and 2 with and without BS cooperation. The CDF for i.i.d. Gaussian random matrices scaled by the average channel gains for each BS and MS are also shown for comparison.

when the MS lacks a dominant link to a single BS can be more emphatically demonstrated using a simple analysis involving two quantities. The first is the ratio of the average cooperative capacity to the average capacity of the best BS-to-MS link. The second is the *3GPP geometry factor*, which is defined as the ratio of the power received on the best BS-to-MS link to the sum of the noise and the powers received on the other links [20], [21]. However, we are interested in using this metric to quantify the relative channel gains from each BS to the MS, and therefore we exclude the noise in our analysis. Mathematically, if $\beta_{\rm P} = \beta_{i_{\rm m}}$ (see (1)), then

$$\text{Geometry Factor} = \frac{\beta_{i_{\rm m}}}{\sum_{i \neq i_{\rm m}} \beta_i}. \tag{3}$$

Figure 5 plots the joint probability density function (pdf) of these two quantities for the combined data from the two routes. This result clearly shows that when the geometry factor is near 0 dB indicating that all three BSs have similar gains to the MS, the cooperative communication provides significant gain. However, when the geometry factor is large indicating a dominant BS-to-MS link, cooperative communication provides little capacity benefit.

Figure 6 plots the cumulative distribution function (CDF) of the average capacities achieved for both the best BS-to-MS link and for cooperative communication using the combined data for both routes, a result that shows significant benefit of BS cooperation. In fact, for this combined data the average capacity resulting from BS cooperation is 53% higher than that achieved using the best BS-to-MS link.

To investigate the observation made in the analysis of Fig. 5 that gain imbalance in the three BS links plays a critical role in determining the capacity, we also scale the elements of the i.i.d Gaussian channel matrix $\mathbf{H}_{\rm iid}$ by the gains computed from the observed channels. Specifically, we 1) scale the columns of $\mathbf{H}_{\rm iid}$ by the gain averaged over all receive antennas and frequencies for each BS antenna and 2) scale the rows of $\mathbf{H}_{\rm iid}$ by the gain averaged over all transmit antennas and frequencies for each MS antenna. Mathematically, we have $\mathbf{H}_0 = \mathbf{R}_{\rm M}^{1/2}\mathbf{H}_{\rm iid}\mathbf{R}_{\rm B}^{1/2}$, where $\mathbf{R}_{\rm M}$ and $\mathbf{R}_{\rm B}$ are diagonal matrices whose diagonal elements represent the average channel power gain for each MS and BS antenna, respectively. Note that this is consistent with the well-known Kronecker model for the channel spatial covariance [22] where $\mathbf{R}_{\rm M}$ and $\mathbf{R}_{\rm B}$ are receive and transmit correlation matrices, respectively. However, choosing these as diagonal matrices enforces zero correlation among the channel transfer functions at the different antennas, a model previously used for antenna arrays with inter-element separation exceeding four wavelengths [23]. The CDF of the capacity resulting from these scaled i.i.d. matrices is compared to that of the measured channel in Fig. 6. As can be seen, scaling by the average gain per BS antenna (assuming $\mathbf{R}_{\rm M} = \mathbf{I}$) leads to an excellent match to the measured capacity. Further comparison between the capacity achieved with the BS-scaled i.i.d. matrices and that obtained using the measured channels shows that they differ by less than 1% at each location. This highlights the dominant influence of channel gain imbalance on the capacity performance for cooperative BS signaling and indicates that the Kronecker correlation model with diagonal transmit and receive correlation matrices works well in this type of cooperative BS environment.

In contrast, the scaling by the average MS gains (assuming $\mathbf{R}_{\rm B} = \mathbf{I}$) results in a capacity that is close to the average capacity predicted by i.i.d. channels without scaling (indicated by the black triangle in Fig. 6). This is an indication that the average channel gains for different MS antennas are similar, despite the fact that the MS antennas include both vertical (V) and horizontal (H) polarizations. To investigate this further, for transmission from the jth BS we compute the ratios $\gamma_{pq}^{(j)} = |H_{pj}|^2/|H_{qj}|^2$, where we have dropped the frequency index notation for convenience. Table II presents the average of several values of $\gamma_{pq}^{(j)}$, where we use the notation V/V (H/H) to indicate that p and q are the indices associated with the two vertically-polarized (horizontally-polarized) MS antennas

Table II
AVERAGE CHANNEL POWER GAIN RATIOS FOR V- AND H-POLARIZED ANTENNAS ON THE MS

	Route 1 (dB)			**Route 2** (dB)		
	V/V	V/H	H/H	V/V	V/H	H/H
BS 1	0.93	3.0	0.44	1.1	2.5	1.1
BS 2	1.1	2.2	0.56	1.6	1.1	0.60
BS 3	1.4	2.5	0.96	1.1	2.5	1.4

and the notation V/H to indicate the average over the four combinations where p and q are associated respectively with vertically- and horizontally-polarized MS antennas. While clearly the gain for the vertical polarization is higher than that for the horizontal polarization, the imbalance is relatively small, confirming our postulation that the channel gains for the different MS antennas are similar.

IV. MULTI-USER SIGNALING

The point-to-point analysis detailed in Section III reveals a number of interesting aspects regarding the cooperative MIMO channel. However, practical cellular systems support multiple users, and it is therefore intriguing to explore the performance impacts associated with multiple cooperative BSs communicating with multiple MSs. We will first consider the downlink channel (BC) and then focus our attention on the uplink channel (MAC) [5].

Throughout this analysis, we focus on K MSs on the measurement routes. Since the data was obtained for a single mobile node, this means that we use channels measured at different times to obtain the required channel data from the BSs to the spatially-displaced users. Naturally, the channel is not strictly static over the time interval between these two measurements, and therefore the performance we obtain does not generally represent the instantaneous performance that would be obtained for K simultaneous links. However, the focus of this analysis is to explore statistical trends over an ensemble of situations. Since the major scattering environment (buildings, parked vehicles, etc.) does not change over the measurement times, this study provides statistically representative multi-user performance behavior.

We assume that each MS only receives or transmits a single data stream, and therefore uses multiple antennas only for diversity or beamforming. While it is possible to also allow each MS to receive or transmit multiple simultaneous streams (multiplexing), inclusion of this capability is of limited value in this study since 1) the cooperative BSs only have three antennas in total, so that even with $K = 2$ only one MS can accommodate multiple streams, 2) all of the various configurations used in the comparative study can support a single stream (but not necessarily multiple streams), and therefore this allows for fair comparisons, and 3) inclusion of multi-stream communication adds complexity without providing detailed additional understanding regarding the trends enabled by the cooperative communication.

The channel normalization is similar to that used for the single-user analysis. However, in this case of multiple users, we must preserve the differences in channel gain to each MS. If the $N_\mathrm{r} \times N_\mathrm{B}$ channel matrix from the BSs to the kth MS at the fth frequency is $\widehat{\mathbf{H}}^{(k)}[f]$ with ith column $\hat{\mathbf{h}}_i^{(k)}[f]$, we scale the matrices for all MSs as $\mathbf{H}^{(k)}[f] = \sqrt{N_\mathrm{r}/\beta_\mathrm{M}}\,\widehat{\mathbf{H}}^{(k)}[f]$ where

$$\beta_\mathrm{M} = \max_{k,i} \left\{ \frac{1}{N_\mathrm{f}} \sum_{f=1}^{N_\mathrm{f}} \left\| \hat{\mathbf{h}}_i^{(k)}[f] \right\|_F^2 \right\}. \tag{4}$$

Note that in the following we drop the frequency index $[f]$ for notational simplicity, recognizing that all sum rate results represent averages over the N_f frequencies.

A. BC Topologies

For the BC, the N_B cooperative BSs apply a beamformer to the signal for the kth MS represented by the $N_\mathrm{B} \times 1$ vector $\mathbf{b}_k$, where the nth element of the vector is the complex weight applied to the signal from the nth BS. The kth MS then applies a beamformer represented by the $N_\mathrm{r} \times 1$ unit-norm vector $\mathbf{w}_k$ to the received signal. If the additive noise at each receiver is modeled as a zero-mean, unit-variance complex Gaussian random process, the sum rate experienced for this BC is [24], [25]

$$C_\mathrm{BC} = \sum_{k=1}^{K} \log\left(1 + \rho_k\right), \tag{5}$$

where

$$\rho_k = \frac{|\mathbf{w}_k^\dagger \mathbf{H}^{(k)} \mathbf{b}_k|^2}{1 + \sum_{i \neq k} |\mathbf{w}_k^\dagger \mathbf{H}^{(k)} \mathbf{b}_i|^2}. \tag{6}$$

We assume that the total transmit power P among all BS antennas is constrained to be a constant such that [24]

$$P = \sum_{k=1}^{K} \mathbf{b}_k^\dagger \mathbf{b}_k. \tag{7}$$

With the normalization of (4) and given that we have assumed Gaussian noise with unit variance, this total power P can once again be considered the SISO SNR to the strongest BS-to-MS link. Also, implicit in this assumption is that the BSs use power control and can change their power allocation up to a total of P. While we could adopt a per-antenna power constraint so that all BSs transmit the same power [26]–[28], our observation matches that of other studies [27] that while this per-antenna constraint slightly reduces the capacity, the resulting trends match those obtained with the sum power constraint. As a result, we use the simpler sum power constraint of (7) in the analysis.

1) MISO Signaling: We first assume that each MS receives using only one of the vertically-polarized antennas in a multiple-input single-output (MISO) configuration. Assigning this antenna to be antenna #1, we have $\mathbf{w}_k = [1, 0, 0, 0]^T$ for each MS, where $\{\cdot\}^T$ indicates a transpose.

Maximum Power Pairing: As a reference case, each mobile user establishes a link with the BS for which the BS-to-MS gain is maximum, even if multiple MSs share the same BS. Therefore, each transmit beamformer $\mathbf{b}_k$ has only a single non-zero entry of value $\sqrt{P/K}$. However, this simple reference case is at a strong disadvantage since it does not benefit from intelligent spatial processing capabilities and therefore can create significant interference at each MS. Motivated by

this observation, *for this case only* we also compute the sum rate when the K MSs equally divide the communication time (time division multiple access or TDMA). In this case, each beamformer has a single non-zero entry of value $\sqrt{P}$, the second term in the denominator of (6) is zero, and we scale (5) as C_{BC}/K. The final reference sum rate for this technique is given as the maximum of the rates computed with and without TDMA.

Optimal Pairing: While pairing each MS to a BS based on the maximum channel gain is simple, it will certainly not maximize the network sum rate. We therefore explore a second reference scenario in which we compute the sum rate for each possible BS-MS pairing and select the pairing that achieves the largest sum rate. Once again, the transmit beamformer for each MS has only a single non-zero entry of value $\sqrt{P/K}$. However, this situation implies additional cooperation, since the network must know the CSI from all BSs to each MS to determine this optimal pairing.

RCI: Finally, we consider a true cooperative MISO BC where the beamformer $\mathbf{b}_k$ for each MS is selected to achieve an appropriate balance of high signal strength for the kth MS and low interference for the other MSs. To construct the beamforming vectors, we use the iterative regularized channel inversion (RCI) method that, assuming the correct initial conditions, achieves optimal sum rate under the constraint of linear processing [24], [25], [29]. For our work, we initiate the iteration using the transmit beamformers obtained for the optimal pairing. This is not guaranteed to converge to the absolute optimum, but does show the improvement possible using a practical beamforming algorithm.

It should be noted that improved performance can be obtained by using non-linear processing known as dirty paper coding (DPC) [5], [30]. While DPC will achieve higher capacity, the capacity difference in most cases is relatively minor, and the trends with channel conditions for DPC and RCI beamforming are similar [24], [31]. To avoid the complex encoding and decoding process associated with DPC and to be consistent with the other linear processing assumed throughout this paper, we choose to use the simpler RCI for our comparative study.

2) MIMO Signaling: Because we have multiple antennas at each MS, we can also explore the BC when these antennas are used. In this case, we use the same scenarios as outlined above for the MISO case. However, we assume that the kth MS knows (through training) the effective channel $\mathbf{H}^{(k)}\mathbf{b}_i$ for $1 \leq i \leq K$ and can therefore construct a minimum-mean-squared error (MMSE) beamformer from [29]

$$\mathbf{w}_k = w_0 \left[\mathbf{I} + \sum_{i \neq k} \mathbf{H}^{(k)} \mathbf{b}_i \mathbf{b}_i^{\dagger} \mathbf{H}^{(k)\dagger} \right]^{-1} \mathbf{H}^{(k)} \mathbf{b}_k, \qquad (8)$$

where w_0 is chosen so that the vector has unit norm. For the iterative RCI algorithm, a new MMSE beamformer for the receiver is computed at each step of the iterative computation. Furthermore, to pair each MS with the BS for which the gain is highest, we select the BS associated with the column of $\mathbf{H}^{(k)}$ that has the highest norm.

B. MAC Topologies

Optimal Pairing: The multiple access channel results when multiple MSs transmit simultaneously and uncooperatively to the cooperative BSs. As a reference case, we assume that each MS transmits from antenna #1 and that the BSs cannot coherently cooperate. For each possible pairing between the kth MS and the nth BS, we compute the sum rate from (5) with

$$\rho_k = \frac{P|H_{1n}^{(k)}|^2}{1 + P\sum_{i \neq n} |H_{1i}^{(k)}|^2}, \qquad (9)$$

where $H_{mn}^{(k)}$ is the mnth element of $\mathbf{H}^{(k)}$ and each MS transmits a power of P. The pairing that achieves the best sum rate is selected as the reference topology.

Cooperative BS: To formulate the capacity when BS cooperation is considered, we let the $N_{\mathrm{B}} \times 1$ vector $\mathbf{z}_m^{(k)}$ represent the mth column of $\mathbf{H}^{(k)T}$. If we continue to assume that each MS transmits from antenna #1, we can construct the $N_{\mathrm{B}} \times K$ channel matrix $\mathbf{Z}$ whose kth column is $\mathbf{z}_1^{(k)}$. Since the MSs cannot cooperate, the capacity for cooperative BSs is equivalent to the point-to-point capacity for an uninformed transmitter based on the composite channel matrix $\mathbf{Z}$, or

$$C_{\mathrm{MAC}} = \log_2 \left[\mathbf{I} + P\mathbf{Z}\mathbf{Z}^{\dagger} \right]. \qquad (10)$$

Cooperative BS/Tx Diversity: Finally, to explore the benefit of exploiting the multiple antennas at each MS, we apply transmit selection diversity, where each MS selects the antenna that achieves the maximum signal strength at the BSs, in addition to the cooperative BS processing. To accomplish this, for each MS we select the value of m that maximizes the norm of the vector $\mathbf{z}_m^{(k)}$, $1 \leq m \leq N_{\mathrm{r}}$. The vector $\mathbf{z}_m^{(k)}$ is used in place of $\mathbf{z}_1^{(k)}$ when constructing the channel matrix $\mathbf{Z}$ for use in (10).

C. Results

The computational results for these multi-user signaling strategies based on the measured data use $K = 2$ or $K = 3$ MSs and an average SISO SNR of 10 dB. The data exhibits a coherence bandwidth, defined here as the frequency separation at which the correlation coefficient of the data falls below 10%, of at least 1 MHz, and therefore to save computational burden the sum rate is computed at 1 MHz intervals over the full bandwidth and averaged in frequency.

Given the large set of possible combinations of locations for the different MSs, we must select a multi-user scenario to use in the analysis. Referring to Fig. 2, the first MS, designated as MS_1, moves along the entirety of routes 1 and 2. The remaining MSs are either at *point 1* or *point 2* which are respectively 700 m or 900 m from the starting point along route 2, locations that allow these MSs to observe multiple BSs. Specifically, when $K = 2$, simulations are run for the second MS (MS_2) at both points, while when $K = 3$, MS_2 is at point 1 while MS_3 is at point 2.

1) BC Topologies: Before studying composite sum rate statistics for the presented scenario, we investigate the sum rate as MS_1 moves along route 1 between the displacements of 200 m and 1000 m with MS_2 at point 1 to allow discussion of

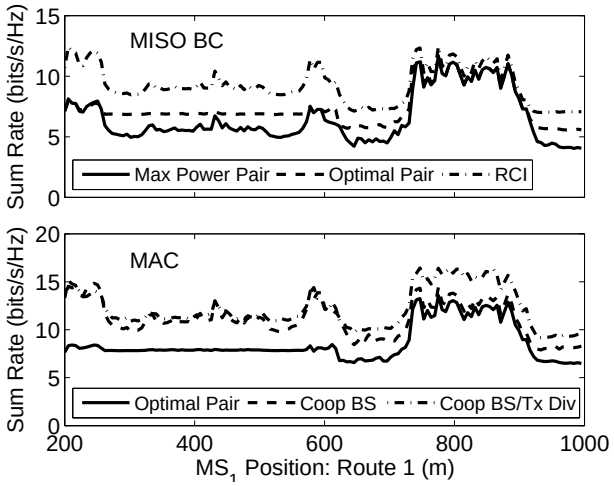

Figure 7. Sum rates computed for different MISO BC and MAC signaling approaches when MS_1 travels along a portion of route 1 and MS_2 is at point 2. The SISO SNR is 10 dB.

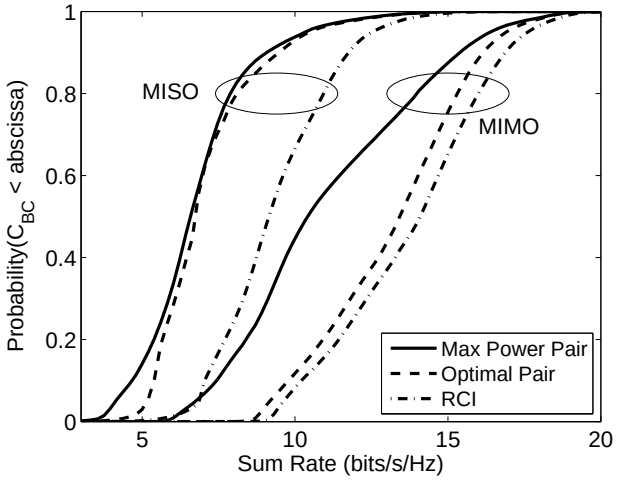

Figure 8. CDF of the sum rate achieved for different MISO and MIMO BC signaling approaches when MS_1 travels along the entirety of routes 1 and 2 and MS_2 is either at point 1 or point 2. The SISO SNR is 10 dB.

the impact of different propagation characteristics on the sum rate. The top plot in Fig. 7 plots the sum rate achieved assuming BC MISO signaling for the three topologies discussed in Section IV-A1, where the data has been smoothed as discussed in Section III. We first observe that the maximum power pairing works well compared to the optimal BS-MS pairing when MS_1 is on the main roads (e.g. between displacements of 750 and 900 m) and enjoys nearly LOS (or strong urban canyon) propagation and therefore a dominant link with a single BS. However, when MS_1 deviates into a small "inlet" (e.g. between displacements of 250 and 550 m), the maximum power pairing increases the multi-user interference, and therefore a different pairing that reduces interference is beneficial. We emphasize that in these interference-limited scenarios, the maximum power pairing would suffer significant additional degradation were it not for the ability to switch to TDMA. But we also note that in a few cases (not shown), the TDMA capability allows the maximum power pairing to outperform the optimal pairing. Finally, since the link gain for two or more BSs to a single MS is similar in these regions, allowing the multiple BSs to collaborate to control interference and maximize link gains through application of the RCI beamforming weights provides significant additional sum rate capability.

Figure 8 plots the cumulative distribution function (CDF) of the data using both MISO BC and MIMO BC signaling (Sections IV-A1 and IV-A2) for $K = 2$ MSs, with the statistics computed by concatenating the simulations for MS_2 at points 1 and 2. It is intuitive that having multiple antennas at the receivers (MIMO BC) enables an increase in the average sum rate. However, these results also show that for MIMO BC signaling, the optimal pairing provides a sum rate approaching that achieved using the full RCI beamforming. This situation occurs because each MS uses knowledge of the transmit beamforming weights to construct its own MMSE receive beamforming weights and therefore is able to suppress the bulk of the interference. This is in contrast to the case of MISO BC signaling, where the receiver is unable to use array signal processing for interference suppression. As a result, the benefit of cooperative transmission is generally less significant for MIMO BC signaling with this optimal pairing, although it should be again emphasized that such optimal pairing requires significant network cooperation and that the multi-antenna reception requires additional complexity at each MS. In most networks, achieving this level of complexity is more feasible in the infrastructure (BS) rather than in the MSs. Therefore, these results reveal that BS cooperation is an effective technique for dramatically improving the performance.

Figure 9 shows the CDF obtained when $K = 3$ MSs for MISO BC signaling. Because $N_{\mathrm{B}} = 3$, communicating with three MSs uses all of the spatial resources available from the cooperative BSs. In this case, the average sum rate achieved with cooperative transmission (RCI) is 91% higher than that achieved with maximum power pairing. This compares with a relative increase of 37% for the two-user scenario considered in Fig. 8. Furthermore, because of the increased interference created by simultaneous transmissions to three different MSs, using the optimal pairing provides some benefit over the maximum power pairing, although it still naturally falls far short of what is achievable using full BS cooperation.

2) MAC Topologies: The bottom plot in Fig. 7 provides the sum rate for the uplink (MAC) scenarios detailed in Section IV-B as MS_1 moves along route 1 between the displacements of 200 m and 1000 m with MS_2 at point 1. Once again, we observe significant performance benefit when the base stations can cooperate in the multi-user reception. Interestingly, when Rx_1 is between the displacements of 200 and 700 m, which is where cooperation tends to give the most benefit, using transmit selection diversity offers little additional benefit. This occurs because the signal processing achieved by the cooperative receivers (BSs) already leverages the diversity in the channels. However, over the region from 750 to 900 m, where cooperation is less beneficial because each MS has a dominant link to a different BS, the use of transmit diversity to overcome fast fading is highly effective.

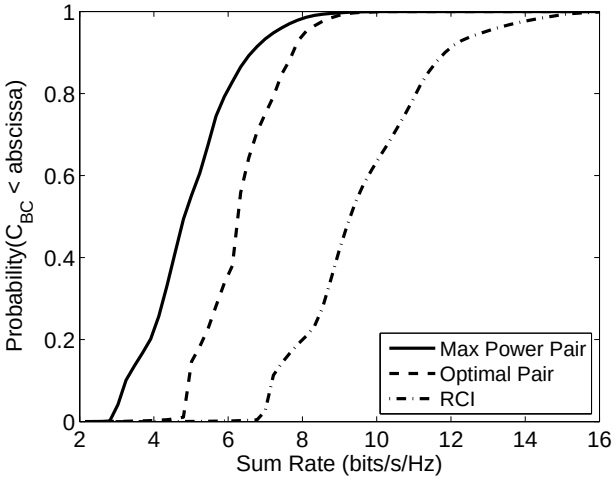

Figure 9. CDF of the sum rate achieved for different MISO BC signaling approaches when MS_1 travels along the entirety of routes 1 and 2 and MS_2 and MS_3 are at two different points along route 2. The SISO SNR is 10 dB.

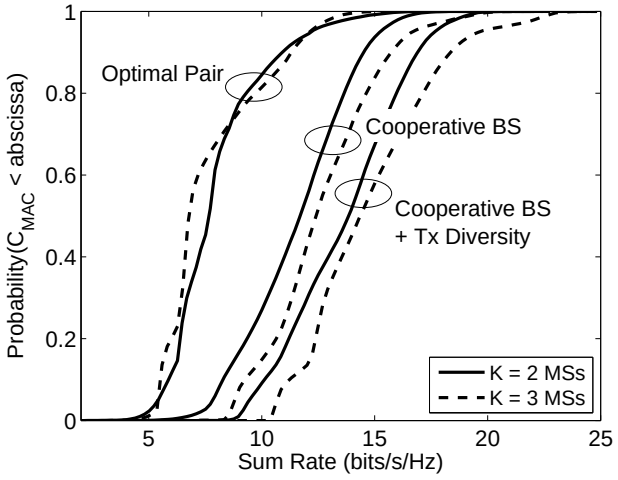

Figure 10. CDF of the sum rate achieved for different MAC signaling approaches when MS_1 travels along the entirety of routes 1 and 2 and MS_2 and MS_3 (if applicable) are at one of two different points along route 2. The SISO SNR is 10 dB.

Finally, Fig. 10 shows the CDF of the sum rate achieved for the uplink scenarios for both $K = 2$ and $K = 3$ MSs. These results reveal increases in the average sum rate of 44% and 63% achieved for 2 and 3 MSs, respectively, assuming only a single antenna used at each MS (no transmit diversity). Perhaps the most striking observation is that the average rate achieved for $K = 3$ MSs is only slightly higher than that achieved for $K = 2$ MSs. This occurs because the impact of the increased total power transmitted is partially offset by the increased interference when $K = 3$, particularly when only one or two BSs experience a strong link to the MSs. The effect is particularly dominant when using optimal pairing since in this technique the BSs cannot cooperate to reduce the multi-user interference, and as a result the sum rate for $K = 3$ MSs is generally lower than that for $K = 2$ MSs. When all three BSs experience a strong link to the MSs and coherent cooperation is allowed, then the sum rate achieved for $K = 3$ is much larger than that for $K = 2$, as evidenced by the differences in the two curves at the high sum-rate levels (upper portion of the curves). Unfortunately, such situations are rare, which is why they occur at relatively low probability.

V. Conclusions

This paper uses fully-coherent measurements from three BS sites to a single MS in a macrocellular environment to explore the potential gains achievable with cooperative BS communication for single-user and multi-user scenarios. Specifically, computations with the data for point-to-point links demonstrate that the average capacity increases by 53% as a result of cooperative BS communication. The analysis further shows that the capacity behavior follows that achieved with i.i.d. Gaussian random channel matrices whose columns are properly scaled to achieve the observed BS-to-MS gains. Evaluation of the data with practical BC signaling strategies shows that cooperation between the BSs can increase the average multi-user sum rate by 37% and 91% for two and three MSs, respectively, when each MS has a single antenna. For MAC signaling, the average improvements are 44% and 63% for two and three single-antenna MSs, respectively, with even more gains achievable using multiple antennas at each MS. Such dramatic capacity improvement motivates further study of coherent cooperative communications for macrocellular settings.

References

[1] J. W. Wallace and M. A. Jensen, "Mutual coupling in MIMO wireless systems: A rigorous network theory analysis," *IEEE Trans. Wireless Commun.*, vol. 3, pp. 1317–1325, Jul. 2004.

[2] B. K. Lau, "Multiple antenna terminals," in *MIMO: From Theory to Implementation*, C. Oestges, A. Sibille, and A. Zanella, Eds. San Diego: Academic Press, 2011, pp. 267–298.

[3] M. A. Jensen and J. W. Wallace, "A review of antennas and propagation for MIMO wireless communications," *IEEE Trans. Antennas Propag.*, vol. 52, pp. 2810–2824, Nov. 2004.

[4] D. Gesbert, S. Hanly, H. Huang, S. Shamai Shitz, O. Simeone, and W. Yu, "Multi-cell MIMO cooperative networks: A new look at interference," *IEEE J. Selected Areas Commun.*, vol. 28, pp. 1380–1408, Dec. 2010.

[5] A. Goldsmith, S. A. Jafar, N. Jindal, and S. Vishwanath, "Capacity limits of MIMO channels," *IEEE Trans. Inf. Theory*, vol. 21, pp. 684–702, Jun. 2003.

[6] S. Zhou, M. Zhao, X. Xu, J. Wang, and Y. Yao, "Distributed wireless communication system: A new architecture for future public wireless access," *IEEE Commun. Mag.*, vol. 41, pp. 108–113, Mar. 2003.

[7] V. Jungnickel, M. Schellmann, L. Thiele, T. Wirth, T. Haustein, O. Koch, W. Zirwas, and E. Schulz, "Interference aware scheduling in the multiuser MIMO-OFDM downlink," *IEEE Commun. Mag.*, vol. 47, pp. 56–66, Jun. 2009.

[8] N. Jaldén, P. Zetterberg, B. Ottersten, and L. Garcia, "Inter- and intrasite correlations of large-scale parameters from microcellular measurements at 1800 MHz," *EURASIP J. Wireless Commun. Netw.*, 2007.

[9] M. Alatossava, A. Taparugssanagorn, and V. Holappa, "Measurement based capacity of distributed MIMO antenna system in urban microcellular environment at 5.25 GHz," in *Proc. IEEE Vehicular Technology Conf. Spring*, Singapore, 11-14 May 2008, pp. 430–434.

[10] V. Jungnickel, S. Jaeckel, L. Jiang, U. Krüger, A. Brylka, and C. von Helmolt, "Capacity measurements in a cooperative MIMO network," *IEEE Trans. Veh. Technol.*, vol. 58, no. 5, pp. 2392–2405, Jun. 2009.

[11] S. Jaeckel, L. Thiele, A. Brylka, L. Jiang, V. Jungnickel, C. Jandura, and J. Heft, "Intercell interference measured in urban areas," in *Proc. 2009 IEEE Intl. Conf. Commun.*, Dresden, Germany, 14-18 Jun. 2009, pp. 1–6.

[12] T. W. C. Brown, P. C. F. Eggers, and K. Olesen, "Simultaneous 5 GHz co-channel multiple-input-multiple-output links at microcellular boundaries: interference or cooperation?" *IET Proc. Microw. Antennas Propagat.*, vol. 1, no. 6, pp. 1152–1159, Dec. 2007.

[13] R. Irmer, H.-P. Mayer, A. Weber, V. Braun, M. Schmidt, M. Ohm, N. Ahr, A. Zoch, C. Jandura, P. Marsch, and G. Fettweis, "Multisite field trial for LTE and advanced concepts," *IEEE Commun. Mag.*, vol. 47, pp. 92–98, Feb. 2009.

[14] V. Jungnickel, L. Thiele, T. Wirth, T. Haustein, S. Schiffermüller, A. Forck, S. Wahls, S. Jaeckel, S. Schubert, S. Gäbler, C. Juchems, F. Luhn, R. Zavrtak, H. Droste, G. Kadel, W. Kreher, J. Mueller, W. Stoermer, and G. Wannemacher, "Coordinated multipoint trials in the downlink," in *Proc. 5th IEEE Broadband Wireless Access Workshop (BWAWS), 2009 IEEE GLOBECOM Workshops*, Honolulu, HI, 30 Nov. - 4 Dec. 2009, pp. 1–6.

[15] R. Fritzsche, J. Voigt, C. Jandura, and G. P. Fettweis, "Verifying ray tracing based CoMP-MIMO predictions with channel sounding measurements," in *International ITG/IEEE Workshop on Smart Antennas (WSA'10)*, Bremen, Germany, 23-24 Feb. 2010, pp. 161–168.

[16] R. Irmer, H. Droste, P. Marsch, M. Grieger, G. Fettweis, S. Brueck, H.-P. Mayer, L. Thiele, and V. Jungnickel, "Coordinated multipoint: Concepts, performance and field trial results," *IEEE Commun. Mag.*, vol. 49, pp. 102–111, Feb. 2011.

[17] P. Marsch, M. Grieger, and G. Fettweis, "Field trial results on different uplink coordinated multi-point (CoMP) concepts in cellular systems," in *Proc. IEEE Global Telecomm. Conf.*, Miami, FL, 6-10 Dec. 2010, pp. 1–6.

[18] Y. Selen and H. Asplund, "3G LTE simulations using measured MIMO channels," in *Proc. IEEE Global Telecomm. Conf.*, New Orleans, LA, 30 Nov.-4 Dec. 2008, pp. 1–5.

[19] J. W. Wallace, M. A. Jensen, A. L. Swindlehurst, and B. D. Jeffs, "Experimental characterization of the MIMO wireless channel: Data acquisition and analysis," *IEEE Trans. Wireless Commun.*, vol. 2, pp. 335–343, Mar. 2003.

[20] S. Plass, X. G. Doukopoulos, and R. Legouable, "Investigations on link-level inter-cell interference in OFDMA systems," in *2006 Symposium on Communications and Vehicular Technology*, Liege, Belgium, 23 Nov. 2006, pp. 49–52.

[21] "Analysis for simulation scenario definition to interference mitigation studies," 3GPP TSG RAN WG4, Tech. Rep. Document R4-060117, Feb. 2006.

[22] J. P. Kermoal, L. Schumacher, K. I. Pedersen, P. E. Mogensen, and F. Frederiksen, "A stochastic MIMO radio channel model with experimental validation," *IEEE J. Selected Areas Commun.*, vol. 20, pp. 1211–1226, Aug. 2002.

[23] V. Pohl, V. Jungnickel, T. Haustein, and C. von Helmolt, "The effect of path loss variations on the capacity of MIMO systems," in *Proc. 5th European Personal Mobile Commununications Conference*, Glasgow, UK, 22-25 Apr. 2003, pp. 458–462.

[24] M. Stojnic, H. Vikalo, and B. Hassibi, "Rate maximization in multi-antenna broadcast channels with linear preprocessing," *IEEE Trans. Wireless Commun.*, vol. 5, pp. 2338–2342, Sep. 2006.

[25] A. L. Anderson, J. R. Zeidler, and M. A. Jensen, "Reduced-feedback linear precoding with stable performance for the time-varying MIMO broadcast channel," *IEEE J. Selected Areas Commun.*, vol. 26, pp. 1483–1493, 2008.

[26] S. Shi, M. Schubert, N. Vucic, and H. Boche, "MMSE optimization with per-base-station power constraints for network MIMO systems," in *Proc. 2008 IEEE Intl. Conf. Commun.*, vol. 55, Beijing, China, 19-23 May 2008, pp. 4106–4110.

[27] F. Boccardi and H. Huang, "A near-optimum technique using linear precoding for the MIMO broadcast channel," in *Proc. 2007 IEEE Intl. Conf. Acoustics, Speech, and Signal Processing*, vol. 3, Honolulu, HI, 15-20 Apr. 2007, pp. 17–20.

[28] W. Yu and T. Lan, "Transmitter optimization for the multi-antenna downlink with per-antenna power constraints," *IEEE Trans. Signal Processing*, vol. 55, pp. 2646–2660, Jun. 2007.

[29] Q. H. Spencer, J. W. Wallace, C. B. Peel, T. Svantesson, A. L. Swindlehurst, and A. Gummalla, "Performance of multi-user spatial multiplexing with measured channel data," in *MIMO System Technology and Wireless Communications*. CRC Press, 2006.

[30] G. Caire and S. Shamai, "On the achievable throughput of a multiantenna Gaussian broadcast channel," *IEEE Trans. Inf. Theory*, vol. 49, pp. 1691–1706, Jul. 2003.

[31] J. Lee and N. Jindal, "High SNR analysis for MIMO broadcast channels: dirty paper coding versus linear precoding," *IEEE Trans. Inf. Theory*, vol. 53, pp. 4787–4792, Dec. 2007.

PLACE PHOTO HERE

Buon Kiong Lau (S'00-M'03-SM'07) received the B.E. degree (with honors) from the University of Western Australia, Perth, Australia and the Ph.D. degree from Curtin University of Technology, Perth, Australia, in 1998 and 2003, respectively, both in electrical engineering.

During 2000-2001, he took a year off from his Ph.D. studies to work as a Research Engineer with Ericsson Research, Kista, Sweden. From 2003 to 2004, he was a Guest Research Fellow at the Department of Signal Processing, Blekinge Institute of Technology, Sweden. In 2004, he was appointed a Research Fellow at the Department of Electroscience, Lund University, Sweden. In 2007, he became an Assistant Professor at the Department of Electrical and Information Technology (formerly Department of Electroscience), Lund University, Sweden, where he is now an Associate Professor. During 2003, 2005 and 2007, he was also a Visiting Researcher at the Department of Applied Mathematics, Hong Kong Polytechnic University, China, Laboratory for Information and Decision Systems, Massachusetts Institute of Technology, USA, and Takada Laboratory, Tokyo Institute of Technology, Japan, respectively. His primary research interests are in various aspects of multiple antenna systems, particularly the interplay between traditionally separate disciplines of antennas, propagation channels and signal processing.

Dr. Lau is an Associate Editor for the IEEE TRANSACTIONS ON ANTENNAS AND PROPAGATION and a Guest Editor of the 2012 Special Issue on MIMO Technology for the same journal. From 2007 to 2010, he was a Co-chair of Subworking Group 2.2 on "Compact Antenna Systems for Terminals" (CAST) within EU COST Action 2100.

PLACE PHOTO HERE

Michael A. Jensen (S'93-M'95-SM'01-F'08) received the B.S. and M.S. degrees from Brigham Young University (BYU), Provo, UT, in 1990 and 1991, respectively, and the Ph.D. degree from the University of California, Los Angeles (UCLA), in 1994, all in electrical engineering. Since 1994, he has been at the Electrical and Computer Engineering Department, BYU, where he is currently a Professor and Department Chair. His research interests include antennas and propagation for communications, microwave circuit design, and multi-antenna signal processing.

Dr. Jensen is currently the Editor-in-Chief of the IEEE TRANSACTIONS ON ANTENNAS AND PROPAGATION. Previously, he was an Associate Editor for the IEEE TRANSACTIONS ON ANTENNAS AND PROPAGATION and the IEEE ANTENNAS AND WIRELESS PROPAGATION LETTERS. He has been a member and Chair of the Joint Meetings Committee for the IEEE Antennas and Propagation Society, a member of the society AdCom, and Co-Chair or Technical Program Chair for six society-sponsored symposia. In 2002, he received the Harold A. Wheeler Applications Prize Paper Award in the IEEE TRANSACTIONS ON ANTENNAS AND PROPAGATION in recognition of his research on multi-antenna communication.